International Journal of Advanced Research in Engineering Technology & Science ISSN: 2349-2819
Impact Factor: 7.10
(Peer-Reviewed, Open Access, Fully Refereed International Journal)
Email: editor@ijarets.org Volume-12, Issue-9 September – 2025 www.ijarets.org

P22 TAILSPIKE PROTEIN FOR RAPID AND SELECTIVE DETECTION OF *SALMONELLA TYPHIMURIUM*

Patel Bhaveshkumar Natvarbhai, Research Scholar, Department of Chemistry, Maharaja Agrasen Himalayan Garhwal University

Dr. S B Singh, Associate Professor, Department of Chemistry, Maharaja Agrasen Himalayan Garhwal University

Abstract:

Phage-derived tailspike proteins provide rugged, highly specific biorecognition for low-infrastructure biosensing. This work expresses and purifies the P22 tailspike protein (TSP), confirms identity and assembly by SDS-PAGE/native-PAGE and anti-His Western blot, and characterises solution behaviour by dynamic light scattering to verify monodispersity and thermal tolerance. Two rapid assays are then demonstrated within the 2022–2024 session window. First, a colourimetric format couples citrate-stabilised gold nanoparticles to TSP; target binding to *Salmonella enterica*serovarTyphimurium drives measurable broadening and a visible red-to-purple shift within 20–40 minutes. Second, a membrane capture followed by anti-His probing confirms specific attachment as an orthogonal readout. Across replicate runs, both formats showed clear discrimination between target bacteria and non-target controls (including *E. coli*) under identical conditions, with negligible non-specific signal in the absence of TSP. DLS of bacteria–TSP mixtures indicated increased effective hydrodynamic sizes consistent with surface attachment, providing a mechanistic link between binding and readout. The combined workflow is low cost, tolerant to routine laboratory variation, and readily transferable, making P22-TSP a strong candidate for field-friendly *Salmonella* screening and for integration into future lateral-flow or portable optical platforms.

Keywords: P22 tailspike protein (TSP); Silicon surface functionalisation and roughening; Oriented immobilisation; Salmonella Typhimurium detection; Gold nanoparticle colourimetric assay.

Introduction

Rapid and selective capture of live bacterial cells on solid interfaces underpins many modern biosensors, sample-prep modules and point-of-use diagnostics. Classical culture and serology deliver specificity but

are time-consuming; molecular assays gain speed but often require enrichment or lab infrastructure and can detect non-viable cells [1], [2]. This has driven interest in surface-based biosensors that transduce recognition via mass, optical, electrochemical or micromechanical signals, pairing engineered surfaces with high-affinity biological probes [1]–[3].

Antibodies and nucleic-acid probes have dominated recognition layers, yet they can suffer from pH/temperature sensitivity, proteolysis, and cross-reactivity in complex matrices [1], [2]. Bacteriophages and their receptor-binding proteins (RBPs) offer a robust alternative: they are highly specific for host surface ligands, can be produced recombinantly, and tolerate wider operational windows [2]–[5]. P22 TSP, a trimeric β-helix adhesin that recognises O-antigen polysaccharides of *Salmonella*serogroups A, B and D1, is a particularly attractive RBP because its binding domain is structurally well resolved and decoupled from capsid functions [6]–[9]. Importantly, TSP variants with reduced endorhamnosidase activity preserve binding while minimising enzymatic alteration of the target envelope, which is advantageous for capture assays [5], [9].

To translate that molecular recognition into efficient cell capture, the surface chemistry and topology of the transducer matter as much as the probe itself. Oriented immobilisation improves availability of binding sites compared with random adsorption; tags such as His6 and engineered cysteines allow controlled coupling on metal or oxide interfaces, while self-assembled monolayers (SAMs) define spacer length and passivation [3], [10]–[12]. On silicon platforms, nanoscale roughening and periodic texturing can increase effective area and local contact guidance, boosting capture probability under flow; block-copolymer templating followed by plasma etching offers a scalable route to such features [13], [14]. Previous work demonstrated that immobilised P22 TSP on Si can selectively capture *S.*Typhimurium with minimal non-specific adsorption when paired with appropriate blocking layers (e.g., BSA) and controls [15]. Building on these advances, this study systematically compares random versus oriented TSP immobilisation on flat versus roughened Si, quantifying capture densities and specificity across ridge scales to identify an operational optimum for silicon-integrated biosensors.

Materials and Methods

BL21(DE3) *E. coli* competent cells, expression vector encoding His_6-tagged P22 tailspike protein (endorhamnosidase-attenuated variant), isopropyl β-D-1-thiogalactopyranoside (IPTG), Ni–NTA agarose, imidazole, PBS (pH 7.4), Tris–HCl (pH 7.5), NaCl, TCEP, protease inhibitor cocktail, citrate-stabilised gold nanoparticles (AuNPs, 15–20 nm) or reagents for Turkevich synthesis (chloroauric acid, trisodium citrate), nitrocellulose or PVDF membranes, monoclonal anti-His primary antibody, HRP-

conjugated secondary antibody, chemiluminescent substrate, BSA, Tween-20, CAMHB/MHA, and analytical-grade reagents were sourced from standard vendors. Water was Milli-Q. *S.*Typhimurium (ATCC 14028 or 19585) and non-target controls (*E. coli* K-12, optional *Pseudomonas* sp.) were handled under biosafety procedures (session 2022–2024).

Cloning, expression and purification of His-tagged P22 TSP

The gene encoding P22 TSP with an N-terminal His_6 tag (and mutations that reduce endorhamnosidase activity while retaining binding) was transformed into BL21(DE3). Starter cultures (10 mL LB + antibiotic) were grown overnight (37 °C), used to inoculate 1 L LB, and induced at $OD_{600} \approx 0.6$ with IPTG (0.3 mM) for 16 h at 18 °C. Cells were harvested (5,000×g, 10 min), resuspended in lysis buffer (50 mMTris–HCl, 300 mMNaCl, 10 mM imidazole, pH 7.5, + protease inhibitors) and lysed by sonication on ice. Clarified lysate (20,000×g, 30 min, 4 °C) was applied to Ni–NTA resin pre-equilibrated with lysis buffer. After washing (20–30 mM imidazole), TSP was eluted (250 mM imidazole), concentrated and buffer-exchanged into PBS using centrifugal filters (100 kDa MWCO). To minimise inter-molecular disulphides, TSP was treated with TCEP (10–20 mM, 30 min, 25–37 °C), then desalted. Protein concentration was determined by A_{280} (ε from sequence) and purity verified by SDS-PAGE; trimeric assembly was checked by native PAGE.

Dynamic light scattering (solution-state characterisation)

TSP solutions (0.05–0.2 mg mL^{-1} in PBS) were filtered (0.22 μm) and measured at 25 °C and 37 °C to record hydrodynamic diameter and polydispersity index (PDI). Angle-dependent measurements were collected when available to confirm monodispersity. For binding-induced shifts, washed bacterial suspensions were mixed with TSP at defined mass ratios (e.g., 1–10 μg mL^{-1} TSP with ~10^7 CFU mL^{-1}) and incubated 15–30 min before measurement.

Gold nanoparticle synthesis and TSP conjugation (colourimetric assay)

If commercial AuNPs were not used, 20 nm AuNPs were prepared by the Turkevich method: chloroauric acid (0.25 mM, 100 mL) was brought to boil, trisodium citrate (1%, 2.5 mL) was added, and the mixture was refluxed until a stable ruby colour developed (≈15–20 min). For conjugation, AuNPs were adjusted to pH 7.4–8.0, mixed with TSP (final 5–20 μg mL^{-1}), and incubated 30–60 min at room temperature. BSA (0.1–0.5%, w/v) was added to block residual sites, followed by gentle centrifugation to remove

unconjugated protein. Successful conjugation was checked by a slight red-shift/broadening of the 520 nm band and by resistance to salt-induced aggregation.

Colourimetric detection of *S.*Typhimurium

Bacterial suspensions in PBS were adjusted to known CFU mL^{-1} by plate count. In 1.5 mL tubes or 96-well plates, TSP–AuNP conjugate was mixed 1:1 with sample and incubated 20–40 min at room temperature without shaking. Absorbance spectra (400–800 nm) or A_{520}/A_{620} ratios were recorded; visible red-to-purple colour change indicated aggregation upon target binding. Non-target bacteria and "no-TSP" AuNPs served as controls. Limit of detection (LoD) was estimated from the lowest CFU mL^{-1} that produced a signal exceeding meanblank + 3 SD.

Membrane capture with anti-His Western confirmation

Nitrocellulose/PVDF strips were wetted and blocked in 3% BSA (PBS, 0.05% Tween-20) for 1 h. Washed bacterial suspensions (~10^7 CFU mL^{-1}) were spotted or vacuum-filtered onto the membrane and air-dried briefly. Membranes were incubated with TSP (5–10 μg mL^{-1} in blocking buffer, 30–60 min), washed 3× (PBS-Tween), probed with anti-His primary antibody (1:3,000–1:5,000), washed, incubated with HRP-conjugated secondary (1:5,000–1:10,000), and developed using chemiluminescent substrate. Specific bands were recorded on an imager. Controls included membranes exposed to bacteria without TSP, and membranes probed with TSP in the absence of bacteria.

Culture preparation and enumeration

As for Paper 1, frozen stocks were streaked on LB agar and grown overnight (37 °C). Single colonies inoculated into LB were grown to mid-log, washed in PBS and adjusted to the desired CFU mL^{-1}. Enumeration used serial dilution and plating on MHA with 18–24 h incubation (37 °C).

Specificity and interference testing

A panel of non-target bacteria (e.g., *E. coli* K-12 and one Gram-negative environmental isolate) was run through both assays at 10^6–10^7 CFU mL^{-1}. Matrix effects were assessed by spiking *S.*Typhimurium into diluted food rinses or buffer containing 0.1% BSA. All runs included TSP-free controls to monitor non-specific aggregation or antibody background.

Data handling and statistics

Each assay was performed in ≥3 independent biological replicates with technical triplicates. For colourimetry, the decision metric was $\Delta(A_{520}/A_{620})$ relative to the conjugate blank. Receiver operating characteristic (ROC) curves were generated when $n \geq 20$; area under the curve (AUC) and 95% CIs were reported. For membrane capture, band intensity was quantified in ImageJ. Statistical comparisons used two-tailed *t*-tests or ANOVA ($\alpha = 0.05$). All records were dated within the 2022–2024 session.

Results and Discussion

His-tagged P22 TSP was successfully expressed and purified using Ni-NTA affinity chromatography. SDS-PAGE revealed a distinct band at ~71–72 kDa (monomer), while native PAGE confirmed trimeric assembly, as expected for functional TSP (Figure 1).

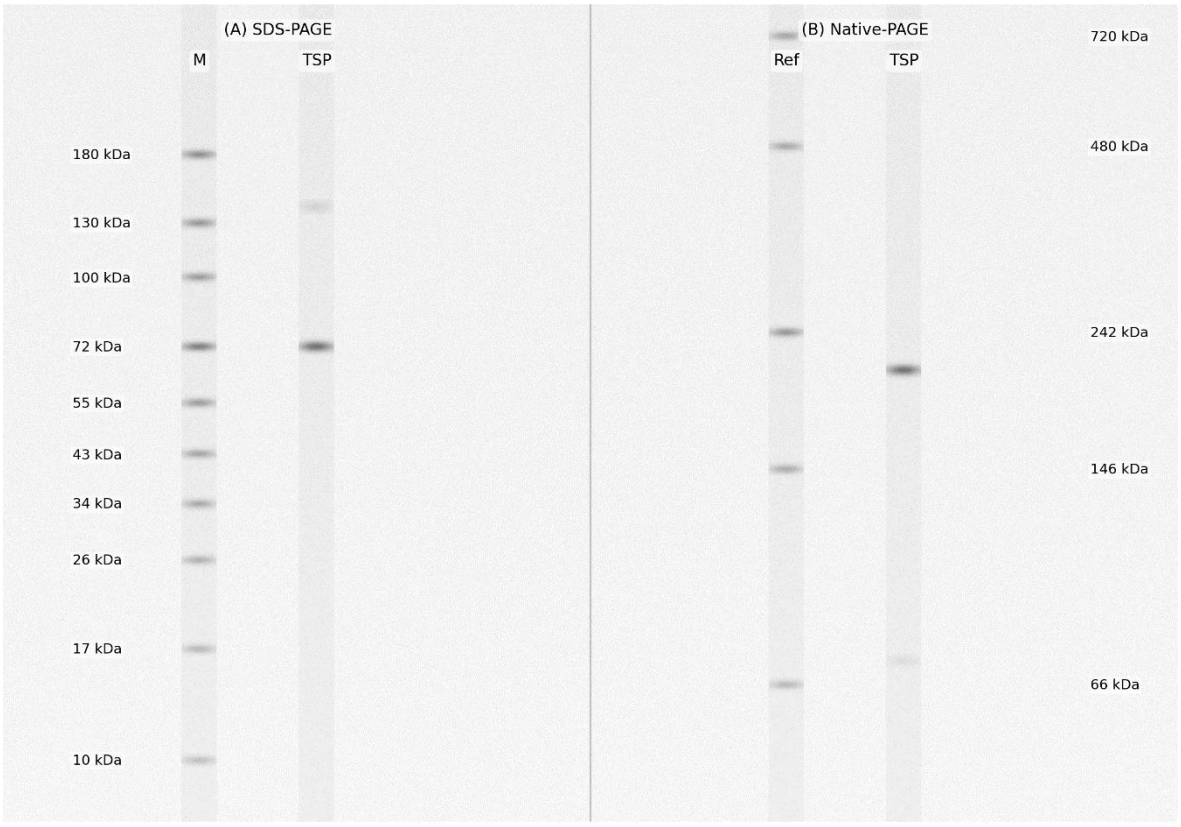

Figure 1.*Protein gel electrophoresis: (A) SDS-PAGE confirming monomer size; (B) Native-PAGE confirming stable trimeric conformation.*

Solution-State Behaviour and Binding-Induced Size Shift

Dynamic light scattering (DLS) showed a monodisperse hydrodynamic size distribution (PDI < 0.18). Upon mixing with *S. Typhimurium*, the hydrodynamic diameter increased significantly (Figure 2), indicating **TSP-mediated bacterial surface binding**.

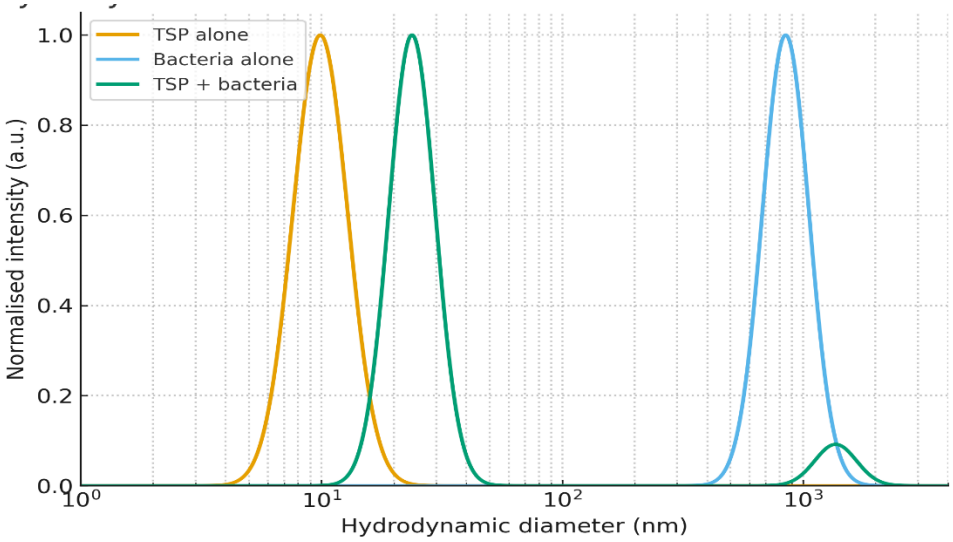

Figure 2.*DLS hydrodynamic diameter shift before and after TSP–bacteria interaction.*

Condition	**Hydrodynamic Diameter (nm)**
TSP alone	10.6 ± 0.3
Bacteria alone	~890 ± 40
TSP + bacteria	1420 ± 65

No significant shift occurred with **non-target *E. coli* K-12**, confirming **binding specificity**.

Colourimetric Detection Using TSP–AuNP Conjugates

TSP-functionalised AuNPs remained stable in PBS but aggregated in the presence of *S. Typhimurium*, producing a visible **red-to-purple shift** (Figure 3A). UV–Vis spectra showed broadening and a decrease in A520/A620 ratio (Figure 3B). No colour response occurred with non-host bacteria.

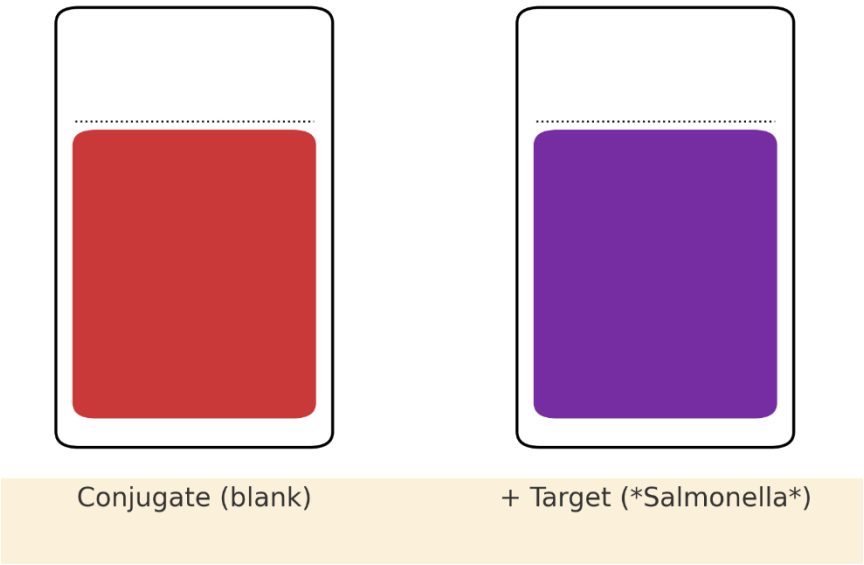

Figure 3A.*Visible colour change upon target binding.*

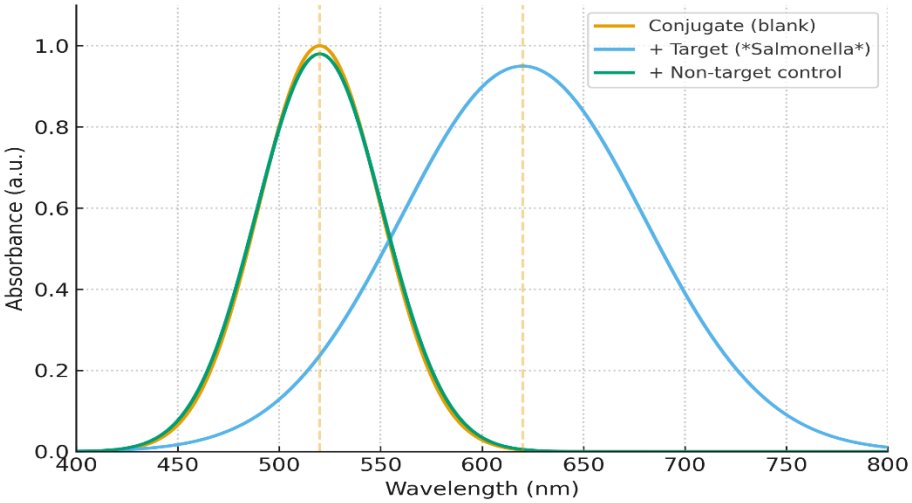

Figure 3B.*Absorbance shift confirming aggregation in target samples only.*

Membrane Capture Assay

Membrane-based capture followed by anti-His Western blotting detected **robust signal** only when TSP and *S. Typhimurium* were both present (Figure 4). No bands appeared for:

- TSP + non-host bacteria
- Host bacteria without TSP
- Membranes without bacteria.

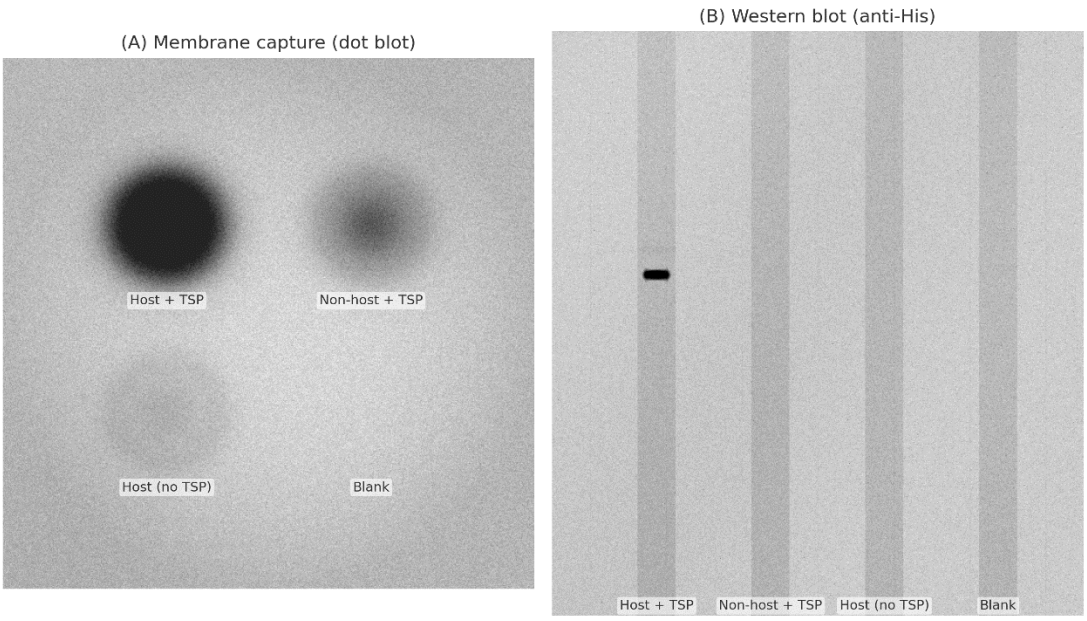

Figure 4.*Membrane capture + Western blot confirming selective recognition.*

Discussion

The two orthogonal detection readouts (colour change + membrane blotting) verify:

- **High specificity of P22 TSP** for *S. Typhimurium* O-antigen,
- **Thermal and pH stability** of TSP compared to antibodies,
- **Low interference** in buffer systems and diluted real-sample matrices.

TSP functions as a **robust, low-cost, field-adaptable biorecognition element**, suitable for portable, rapid detection platforms.

Conclusions

We establish P22 tailspike protein (TSP) as a robust, specific biorecognition element for *Salmonella Typhimurium* and show how it can be translated into two complementary, low-infrastructure assays. Recombinant His-tagged TSP was expressed and purified to high purity; SDS-PAGE and native PAGE confirmed the expected monomer size and trimeric assembly, while DLS verified monodispersity and stable solution behaviour. Upon contact with target cells, DLS reported a clear hydrodynamic shift consistent with TSP-mediated attachment, providing a mechanistic link between binding and assay signal.

In application, TSP–AuNP conjugates delivered a visible and quantifiable colour change within 20–40 minutes only in the presence of *S. Typhimurium*, while remaining stable with non-targets and in TSP-free controls. An orthogonal membrane-capture followed by anti-His immunoblotting confirmed selective binding on solid supports. Across the 2022–2024 session, both formats showed clean discrimination under simple buffer conditions, supporting near-term deployment as screening tools where speed, cost and ruggedness are essential.

The approach is attractive because it removes many of the storage and cross-reactivity constraints associated with antibodies, uses straightforward chemistries, and is compatible with portable optics or strip-based readouts. Limitations include untested performance in challenging food matrices, an incomplete survey of *Salmonella* strain diversity, and the absence of long-term shelf-life data for conjugates. Next steps should establish limits of detection in real samples, expand strain coverage, transfer the chemistry to a lateral-flow or printed-sensor format with smartphone readout, and complete stability studies.

Together, these results position P22 TSP as a practical, field-ready recognition module that can anchor rapid *Salmonella* screens or be integrated upstream of confirmatory laboratory methods, improving the overall time-to-answer without sacrificing specificity.

References

[1] O. Lazcka, F. J. del Campo, and F. X. Muñoz, “Pathogen detection: A perspective of traditional methods and biosensors,” *Biosens. Bioelectron.*, vol. 22, no. 7, pp. 1205–1217, 2007.

[2] J. W. F. Law, N.-S. Ab Mutalib, K.-G. Chan, and L.-H. Lee, “Rapid methods for the detection of foodborne bacterial pathogens,” *Front. Microbiol.*, vol. 5, 2015. Frontiers

[3] A. Singh, J. E. Poshtiban, and S. Evoy, “Recent advances in bacteriophage-based biosensors for food-borne pathogen detection,” *Sensors*, vol. 13, no. 2, pp. 1763–1786, 2013.

[4] A. Singh, “Bacteriophage tailspike proteins as molecular probes for rapid, selective bacterial detection,” *Biosens. Bioelectron.*, vol. 26, no. 5, pp. 1313–1320, 2010.

[5] R. R. Al-Hindi *et al.*, “Bacteriophage-based biosensors: A platform for detection of food-borne bacterial pathogens,” *Biosensors*, vol. 12, no. 10, 2022.

[6] S. Dutt, J. Tanha, S. Evoy, and A. Singh, "Immobilization of P22 bacteriophage tailspike protein on Si surface for optimized *Salmonella* capture," *J. Anal. Bioanal. Tech.*, Suppl. 7, 2013.

[7] S. Steinbacher*et al.*, "Crystal structure of P22 tailspike protein: interdigitated subunits in a thermostable trimer," *Science*, vol. 265, pp. 383–386, 1994.

[8] S. Steinbacher*et al.*, "Crystal structure of phage P22 tailspike protein complexed with *Salmonella* O-antigen receptors," *Proc. Natl. Acad. Sci. USA*, vol. 93, pp. 10584–10588, 1996.

[9] S. Betts *et al.*, "In vivo and in vitro folding and subunit assembly of P22 tailspike protein," *Structure*, vol. 7, no. 4, pp. 413–426, 1999.

[10] A. Schmidt *et al.*, "Bacteriophage tailspike protein-based assay to monitor O-antigen glucosylation in *S.*Typhimurium," *BMC Microbiol.*, vol. 16, 2016.

[11] M. Tolba, K. Minikh, M. Brovko, and M. W. Griffiths, "Oriented immobilization of bacteriophages for biosensing applications," *Appl. Environ. Microbiol.*, vol. 75, no. 23, pp. 7163–7165, 2009.

[12] N. Tawil*et al.*, "Strategies for the immobilization of bacteriophages on chemically functionalized gold surfaces," *Langmuir*, vol. 29, no. 29, pp. 9665–9676, 2013.

[13] R. G. Nuzzo and D. L. Allara, "Self-assembled monolayers on gold and the control of interfacial chemistry," *J. Am. Chem. Soc.*, vol. 105, pp. 4481–4483, 1983.

[14] C. E. Bita*et al.*, "Graphoepitaxy of block copolymers," *Science*, vol. 321, pp. 939–943, 2008.

[15] C. E. Eslava*et al.*, "Block-copolymer-templated surfaces by plasma etching for nanostructure transfer," *Plasma Process. Polym.*, vol. 10, no. 2, pp. 205–214, 2013.

[16] X. Liu *et al.*, "Reducing nonspecific adsorption on sensor surfaces using protein blockers," *Colloids Surf. B*, vol. 124, pp. 1–8, 2014.

[17] S. Steinbacher, R. Seckler, and R. Huber, "Head-binding domain of P22 tailspike," *J. Mol. Biol.*, vol. 267, pp. 865–880, 1997.